HOSTED BY
ELSEVIER
Available online at www.sciencedirect.com
ScienceDirect
Soils and Foundations 62 (2022) 101210
www.elsevier.com/locate/sandf

Technical Note

Hydraulic conductivity test system for compacted, 2-mm-thick bentonite specimens

Daichi Ito [a,*], Hailong Wang [b], Hideo Komine [c]

[a] Department of Civil and Environmental Engineering, Waseda University, Tokyo, Japan
[b] Global Center for Science and Engineering, Waseda University, Tokyo, Japan
[c] Faculty of Science and Engineering, Waseda University, Tokyo, Japan

Received 22 September 2021; received in revised form 25 July 2022; accepted 16 August 2022
Available online 5 September 2022

Abstract

Both the design and safety assessment of radioactive waste disposal facilities demand an accurate evaluation of the hydraulic conductivity of the bentonite materials, especially compacted bentonite. For permeability tests of bentonite materials, the lengthy time necessary for specimen saturation and measurement may present a bottleneck. The permeability behavior of bentonite, such as the effects of the water quality and the exchangeable cations, has not been systematized sufficiently. For the present study, a hydraulic conductivity test system with 2-mm-thick specimens was developed. Its applicability was evaluated in terms of test accuracy. Six specimens of compacted Japanese sodium bentonite, with dry densities of 1.34–1.79 Mg/m^3, were subjected to falling head hydraulic conductivity tests. The results showed that the hydraulic gradient set for this study did not affect the hydraulic conductivity, indicating that the macroscopic hydraulic behavior was consistent with Darcy's law. Furthermore, it was possible to reduce the test period considerably, by about one-tenth, compared to that using 10-mm-thick specimens. The obtained hydraulic conductivity was found to be similar to that in earlier studies. Furthermore, the values showed less variation particularly in terms of the consolidation test results. The results demonstrated that 2-mm-thick specimens are useful for hydraulic conductivity measurements of compacted bentonite.

Keywords: Bentonite; Hydraulic conductivity; Hydraulic gradient; Radioactive waste; Geological disposal

1. Introduction

Compacted bentonite is used as a buffer and backfill material in various radioactive waste disposal facilities worldwide, including facilities for the geological disposal of high-level radioactive waste (Pusch, 1992; JNC, 1999; Komine and Watanabe, 2010; SKB, 2011; Sellin and Leupin, 2013). Buffer and backfill materials must have sufficiently low hydraulic conductivity (k) in order to isolate radionuclides for thousands to tens of thousands of years. The k value of compacted bentonite and sand–bentonite mixtures might be in the order of 10^{-9} m/s or less, depending on the dry density, bentonite and montmorillonite contents, composition of the exchangeable cations, etc. (Gleason et al., 1997; Pusch and Yong, 2006; Komine, 2010; Tanai et al., 2010). In particular, the k of some compacted sodium-type bentonites might be 10^{-11}–10^{-14} m/s (Mesri and Olson, 1971; Achari et al., 1999; Dixon et al., 1999; Siemens and Blatz, 2006; Karnland et al., 2008; Komine, 2008; Wang et al., 2013), for which widely accepted testing methods cannot be directly applied (e.g., ISO, 2004; JIS, 2009; ASTM, 2016). The ISO test standard (ISO, 2004) and ASTM test standard (ASTM, 2016) stipulate the lower limit of applicability as 1×10^{-11} m/s. In

Peer review under responsibility of The Japanese Geotechnical Society.
* Corresponding author at: 58-203, 3-4-1, Okubo, Shinjuku, Tokyo 169-8555, Japan.
E-mail address: daichi_ito@akane.waseda.jp (D. Ito).

https://doi.org/10.1016/j.sandf.2022.101210
0038-0806/

order to measure k lower than 1×10^{-11} m/s, extra steps, such as temperature control, change in the specimen size, and increased accuracy of the equipment, are necessary. For the JIS test standard (JIS, 2009), soil materials with a hydraulic conductivity of 1×10^{-9} m/s or less were treated as fundamentally impermeable materials. No specific measurement method was described. Recently, a new standard (JGS, 2018) was developed to cover permeability in the order of 10^{-9}–10^{-13} m/s with the recent expansion of the use of low-permeability soil materials, including bentonite.

For low-permeability materials, including bentonite, k has often been estimated based on consolidation tests (Mesri and Olson, 1971; Yeo et al., 2005; Butsuda et al., 2006; Ahn and Jo, 2009; Komine, 2021). One benefit of consolidation tests is that the k of the materials is obtainable in a short period of time compared to permeability tests. Butsuda et al. (2006) reported that consolidation tests applying high pressure of up to 10 MPa can quantify k in about 10 days. However, consolidation tests assess the combined behaviors of water advection and specimen compaction. For cases of specimens with a high swelling capacity, such as compacted bentonite, some concerns arise, such as the occurrence of errors, because of wall friction (Tanai et al., 2010).

One bottleneck of the permeability testing of compacted bentonite is the test duration. According to a report on the permeability testing of bentonite materials in Japan, compiled by the JGS Research Committee on the Utilization and Performance Evaluation Technology of Low-Permeability Soil Materials (JGS, 2016), the permeability test specimen size was 50 mm, 60 mm, or 100 mm in diameter. The specimen length was 0.2–1.2 times the diameter. The hydraulic gradient (i) of the specimens ranged from a few dozen to a maximum of about 1,000. The duration of the tests ranged from months to years. In addition, the permeability test duration was estimated based on the test conditions used for earlier studies. Each specimen was made of soil material with a particle density of 2.77 Mg/m^3 and compacted into a cylinder with a diameter of 60 mm, a height of 20 mm, and a dry density of 1.6 Mg/m^3. When the hydraulic conductivity was set at 1×10^{-12} m/s, with i of 1000, about 98 days had to pass in order to obtain a flow volume equivalent to the specimen pore volume (23.9 cm^3). Under the same test conditions, if the height of the specimen was reduced to 10 mm (1/2), then i was doubled. The pore volume was also reduced to 1/2. Therefore, the test period was reduced to 25 days (1/4). When the specimen height was reduced to 5 mm (1/4), the test period was reduced to 6 days (1/16). Consequently, reducing the specimen height can effectively reduce the test duration because of both a reduced pore volume of the specimen and an increased i. Furthermore, in terms of specimen saturation, thinning the specimen makes it easier to saturate the specimen evenly in a short time.

To shorten both the saturation period and the test period by increasing i, a permeability test apparatus with a 2-mm-thick specimen was developed. The k of compacted bentonite was measured. This paper presents the testing procedures and results for specimens with a 2-mm thickness and i of up to 16000.

2. Material and methodology

A commercial bentonite powder, Kunigel V1 (K_V1), was used for this study. It was mined from Tsukinuno Clay Mine, Yamagata Prefecture, Japan. In fact, K_V1 is a promising candidate for use as a buffer material in geological disposal projects in Japan. It has been assessed in many earlier studies (JNC, 1999; Kawamura et al., 1999; Komine and Ogata, 1999; Cui et al., 2008; Komine et al., 2009; Kobayashi et al., 2017; Tanaka and Watanabe, 2019). Table 1 presents the physicochemical properties of K_V1. It contains 52.8 % montmorillonite with dominant exchangeable cations of sodium. Its soil specific gravity, liquid limit, and plastic limit are 2.76, 535.4 %, and 26.7 %, respectively. The initial water content of the material measured for this study was about 9 %. The particles of K_V1 were adjusted to have less than 50 μm (Ito et al., 1994; Wang et al., 2019).

Hydraulic conductivity tests were conducted using the system presented in Fig. 1(a). The system consisted of a test cell, two burettes, and two pressure regulators. For the test cell in Fig. 1(b), each specimen was confined radially by a specimen ring (Fig. 1(c)) and sandwiched between upper and lower plates to restrain the swelling deformation. Burettes with a minimum scale of 0.1 mL and a capacity of 10 mL were used for water inflow and outflow measurements. The burettes were installed in acrylic pipes, by which the water pressure in the burettes could be adjusted through pressure regulators. The top opening of each burette was kept to a minimum level. Then, water was filled through the acrylic pipes to reduce evaporation. Tubes made of polyolefin (2-mm inner diameter) were used to connect the burettes and the test cell because of their good performance at reducing water evaporation through the tube wall. Membrane filters made of polyether sulfone, with a pore size of 0.45 μm and a thickness of 140 μm (Nishimura et al., 2011), were placed at the top and bottom surfaces of the specimen. The value of k for the filter was measured as 2.0×10^{-8} m/s.

Table 1
Physicochemical properties of K_V1.

Soil specific density (−)	2.76
Liquid limit (%)	535.4
Plastic limit (%)	26.7
Plasticity index	508.7
Content of montmorillonite (%)	52.8
Exchangeable cation of Na^+ (cmol/kg)	53.8
Exchangeable cation of Ca^{2+} (cmol/kg)	35.5
Exchangeable cation of Mg^{2+} (cmol/kg)	4.1
Exchangeable cation of K^+ (cmol/kg)	1.6
Accessory minerals	quartz, feldspar, calcite

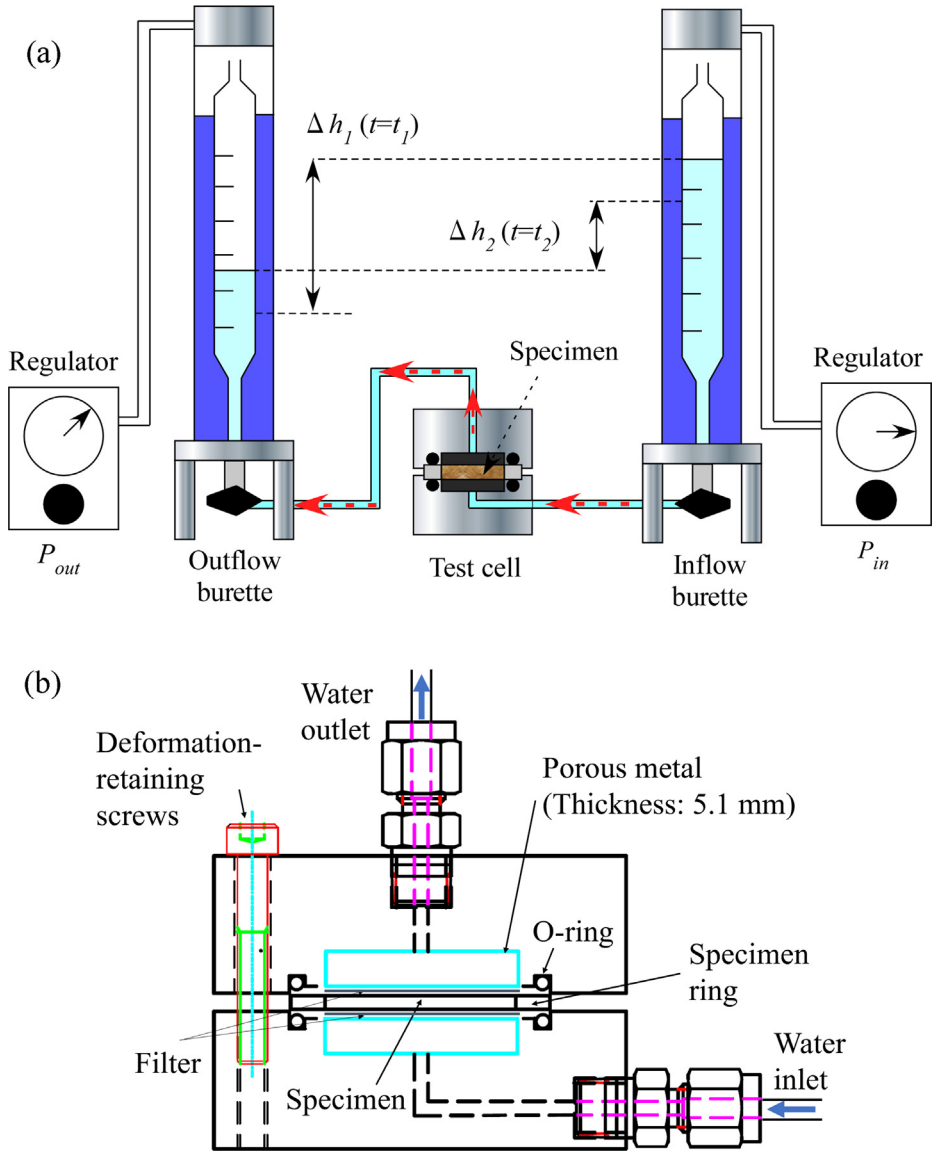

Fig. 1. Test system: (a) illustration of whole test system, (b) cross-sectional view of test cell, and (c) specimen and 2-mm-thick stainless ring.

It should be noted that this testing system does not separate the water flows through the interface between the specimen and the specimen ring. Watanabe et al. (2013) investigated the effect of the local flow near the sides of a specimen on the hydraulic conductivity using Ca-type bentonite and sand mixture specimens. They found that the effect of the local flow near the interface may be about 2 times faster at maximum than that in the specimens. It is expected that this can be attributed to the larger sand particles when comparing the surface roughness of the specimen range and the lower swelling potential of the Ca-type bentonite compared to the Na-type bentonite. The average surface roughness of the specimen ring in this study is 1.6 μm which is larger than the 60 % particle size of K_V1 (Wang et al. 2019). Thus, the interface flow would not be significant. In addition, the height to diameter ratio, representing the ratio of the side wall area to the specimen surface area, is 0.07, much smaller than that of past studies, which also suggests a smaller side wall effect.

Six specimens with a diameter of 28 mm and a thickness of 2 mm, as shown in Table 2, were prepared covering a dry density range of 1.34 – 1.79 Mg/m^3. Another specimen having an equal diameter, but a thickness of 10 mm, was also tested for a comparison of the required times of the flow volume. To prepare each specimen, a predetermined amount of K_V1 powder was directly compacted into the specimen ring. The specimen weight was found using a balance up to 1 μg. The thickness and diameter were measured to the nearest 1 μm during the specimen preparation. This means that the thickness and diameter measurement errors

Table 2
Specimen and test conditions.

Specimen dry density ρ_d (Mg/m^3)	Specimen thickness L (mm)	Applied air pressure at water inflow and outflow sides $\binom{P_{in}}{P_{out}}$(kPa)	Approximate hydraulic gradient i (-)	Pore volume V_v (cm^3)
1.34	2	$\binom{100}{20} \rightarrow \binom{200}{40} \rightarrow \binom{300}{60}$	4,000 → 8,000 → 12,000	0.637
1.51	2	$\binom{100}{20} \rightarrow \binom{200}{40} \rightarrow \binom{300}{60} \rightarrow \binom{400}{80}$	4,000 → 8,000→ 12,000 → 16,000	0.563
1.62	2	$\binom{440}{120}$	16,000	0.523
1.70	2	$\binom{100}{20}$	4,000	0.490
1.77	2	$\binom{100}{20}$	4,000	0.456
1.77	10	$\binom{500}{100}$	4,000	2.21
1.79	2	$\binom{100}{20} \rightarrow \binom{220}{60} \rightarrow \binom{340}{100} \rightarrow \binom{440}{120}$	4,000 → 8,000→ 12,000 → 16,000	0.449

should be less than 1 μm. The specimen dry density was calculated based on the obtained mass, dimensions, and initial water content.

After the specimen was assembled into the testing cell, the cell was immersed in distilled water for a day with the application of negative pressure of approximately −98 kPa for specimen saturation. Then, the cell was connected to the two burettes, carefully ensuring that no air was tramped along the water flow path. Finally, air pressure was gradually applied to the burettes, as presented in Table 2. The applied pressures were changed in several stages for some of the specimens to elucidate the effects of i on the measurements. Additionally, the applied pressures were kept to less than the swelling pressures of the test specimens, referring to the measurement results of 2-mm-thick compacted sodium bentonite specimens by Wang et al. (2022c) to prevent shrinkage deformation. Moreover, the values of the swelling pressure were almost the same for both 2-mm and 10-mm thicknesses (Wang et al., 2022b), and the air pressure loaded on the 10-mm specimen was smaller than the swelling pressure. The room temperature and water levels of the burettes were recorded at arbitrary time intervals.

The value of k at the testing temperature (k_T) was calculated using equation (1) and then converted to a value at 15 °C (k_{15}) with equation (2) based on JGS (2018).

$$k_T = 2 \cdot 303 \frac{(A_{in} \times A_{out})L}{(A_{in} + A_{out})A_{spe}(t_2 - t_1)} \log_{10} \frac{\Delta h_1 \gamma_w + \Delta P}{\Delta h_2 \gamma_w + \Delta P} \quad (1)$$

$$k_{15} = k_T \times \frac{\eta_T}{\eta_{15}} \quad (2)$$

In these equations, the following variables are used: A_{in} and A_{out} stand for the cross-sectional areas of the burettes on the inflow and outflow sides (=0.51 cm^2), respectively, L, A_{spe} expresses the cross-sectional area of the specimen, Δh_1 and Δh_2 signify the water level differences at times t_1 and t_2, respectively, γ_{w} represents the unit volume weight of water, ΔP represents the differential pressure between the inflow (P_{in}) and the outflow (P_{out}), and η_T/η_{15} is the correction factor for calculating k_{15}.

In equation (1), the hydraulic head loss caused by the membrane filters was not considered because the k of the filter is three orders higher than that of the tested specimens. The filter thickness is about one-tenth of the specimen thickness.

3. Test results and discussion

3.1. Time histories of water inflow and outflow

Fig. 2 presents a comparison of the relation between the inflow and outflow of the water normalized by the pore volume and elapsed time for the specimen thicknesses of 2 mm and 10 mm. The same test system was used along with the same dry density (1.77 Mg/m^3), initial water content (9.2 %), and i (4000). The pore volume was found to be 0.456 cm^3 for the 2-mm-thick specimen and 2.21 cm^3 for the 10-mm-thick specimen. For the 2-mm-thick specimen, a large difference was found between the inflow and the outflow immediately after the start of the test. It is noteworthy that the inflow and outflow are well balanced because the water level difference at time t_1 (Δh_1) and that at t_2 (Δh_2) are used in the calculation of k, as shown in equation (1). If a large difference exists between the inflow and outflow during the start of the test for the first measurement, as in the case of the 2-mm specimen shown in this figure, then k is not calculated. However, for the 2-mm-thick specimen, the increased inflow and outflow with time soon became parallel, indicating that they are well balanced. In contrast, for the 10-mm-thick specimen, the increased inflow was larger than the increased outflow until the end of the test. The reason for the lack of balance in the case of the 10-mm specimen is unclear, but it may be because of system compliance or measurement errors, such as evaporation or invisible leakage. To ensure the accuracy of the falling head permeability test, it is necessary to balance the inflow and outflow. It is easier to balance the inflow and outflow of the 2-mm-thick specimen. In the test on the 2-mm-thick specimen, it took nine days for the inflow to equal the pore volume and about 31 days to reach

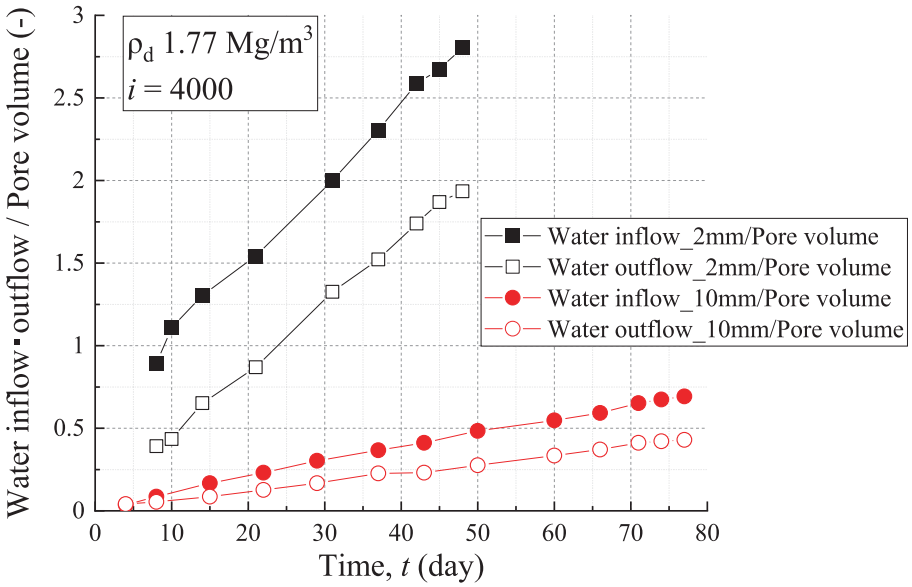

Fig. 2. Relations between time and water volume of inflow and outflow normalized by pore volume for specimen thicknesses of 2 mm and 10 mm.

twice the value. Therefore, the results show that the permeability test period can be shortened considerably by using the test system with a specimen having a 2-mm thickness.

Fig. 3 shows the time course of the water volume of the inflow and outflow normalized by the pore volume for 1.34 Mg/m^3, 1.51 Mg/m^3, 1.62 Mg/m^3, 1.70 Mg/m^3, and 1.79 Mg/m^3. In this figure, the change in i is also shown. Although differences are seen between the inflow and outflow volumes and the slopes of increase in some cases, such as 1.34 Mg/m^3 and 1.70 Mg/m^3, the overall trend is for the inflow and outflow to increase harmoniously. The reason for the lack of balance in the case of 1.34 Mg/m^3 and 1.70 Mg/m^3 is unclear, but it may be because of system compliance or measurement errors, such as evaporation or invisible leakage.

Fig. 4 shows the relation between the Darcy flux (v) and i for the 1.34 Mg/m^3, 1.51 Mg/m^3, and 1.79 Mg/m^3 cases, where v is an averaged value with an error bar for all recorded data under the same i. It can be seen that v is proportional to the increase in i, indicating that the range in tested i (4,000–16,000) does not markedly affect k and satisfies Darcy's law.

Fig. 5 shows the relation between k and i for the 2-mm specimens in this study and that for the 10-mm specimen obtained by Sadamatsu et al. (2020). With a range in i of 3,000 $\sim$ 4,000, the k values for specimens under similar densities are very similar regardless of the specimen thickness. Although it seems there is a decreasing trend for the 1.34 Mg/m^3 and 1.51 Mg/m^3 cases as i increases, this trend is very minor and the tested range in i is reasonable.

Fig. 5 also shows the relation between k and i in a comparison of the experimental cases where the flow volume is more or less than the pore volume in each i phase. For the 1.34 Mg/m^3 and 1.51 Mg/m^3 cases, few differences in k were observed between the phases when the flow volume either exceeded and did not exceed the pore volume. Also, for the 1.79 Mg/m^3 case, the k at each i was almost constant.

3.2. Dry density effect on k

To validate the results obtained from the permeability test system used for this study, Fig. 6 shows the relation between k and the dry density of the compacted K_V1 specimens compared to the results of earlier studies using high-pressure consolidation tests (Butsuda et al., 2006; Komine et al., 2011), a constant head permeability test (Hasegawa, 2004), a falling head permeability test with 10-mm-thick specimens using the same test equipment as that used for this study (Sadamatsu et al., 2020), and the calculated results of theoretical equations for the hydraulic conductivities of the bentonite-based buffer and backfill materials (Komine, 2008). Table 3 shows the test conditions employed in previous studies. In the high-pressure consolidation test, k was calculated according to the JIS test standard for consolidation tests (JIS, 2009) with a maximum consolidation pressure of 10 MPa. A theoretical equation for hydraulic conductivity was developed based on the assumption that water molecules flow laminarly through the montmorillonite crystal interlayers. The theoretical equation was the same as that described in an earlier study (Komine, 2008), considering the composition of exchangeable cations existing between two montmorillonite parallel layers. The properties of bentonite, such as the CEC (cation exchange capacity), EXC (exchange capacity of each exchangeable cation, such as Na^+, Ca^{2+}, K^+, Mg^{2+}), and content of montmorillonite input to the theoretical equations, are shown in Table 1. The input values of the parameters, such as the montmorillonite particle density, non-hydrated radius exchangeable cations, mont-

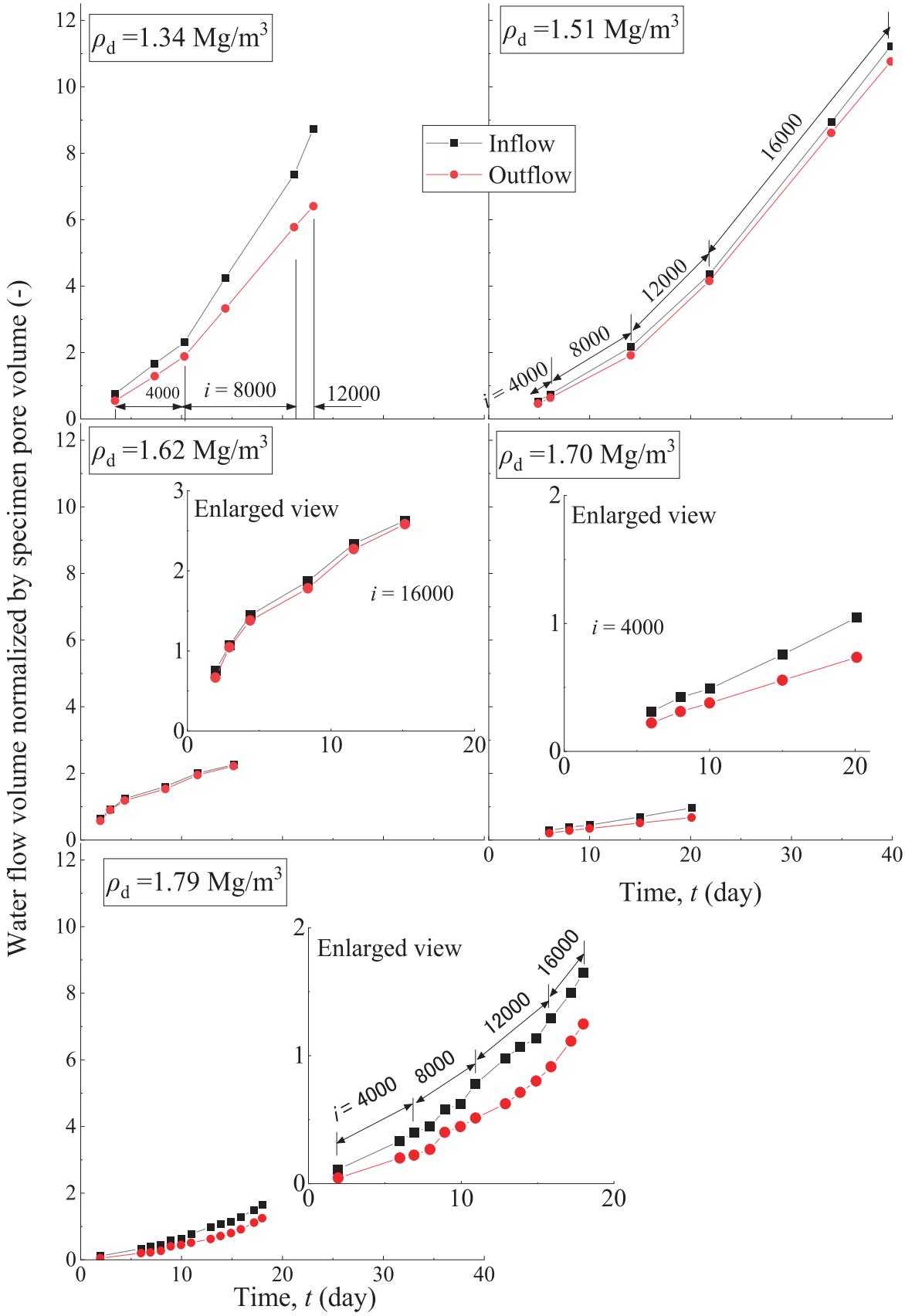

Fig. 3. Time courses of water volume of inflow and outflow normalized by pore volume cases of 1.34 Mg/m^3, 1.51 Mg/m^3, 1.62 Mg/m^3, 1.70 Mg/m^3, and 1.79 Mg/m^3.

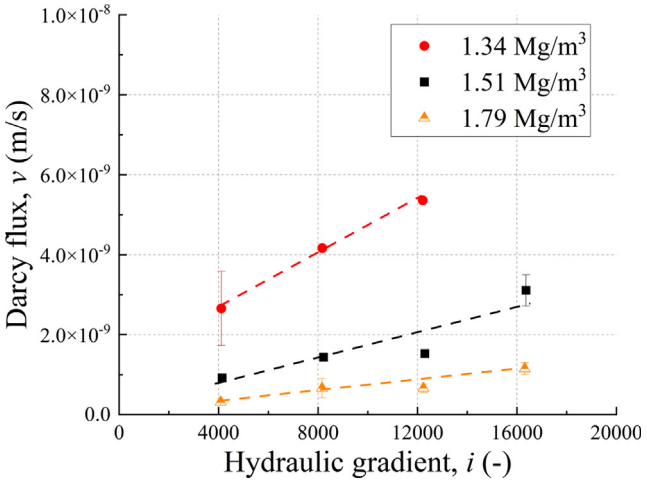

Fig. 4. Relation between Darcy flux v and hydraulic gradient i.

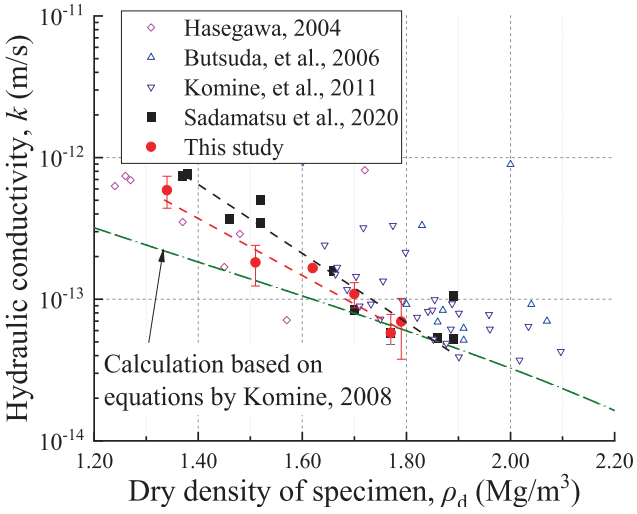

Fig. 6. Comparison with previous studies of relation between hydraulic conductivity and dry density.

morillonite layer thickness, and the coefficient of viscosity of water, were the same as those reported by Komine (2008). The parameter representing the ratio of density and coefficient of viscosity between the interlayer water and the free water (R) was substituted as 79.

As in earlier studies, a negative correlation was found between the normal logarithm of k and the dry density of the specimens, as shown in Fig. 6. Additionally, the relation between the k and the dry density obtained in this study generally shows a similar trend to the trends found in earlier studies. In particular, the results obtained from this study were similar to those obtained using a similar test system with a specimen thickness of 10 mm (black square plot in Fig. 6). Moreover, the values obtained for this study were almost in the middle of the dataset of values obtained in earlier studies. The scattering indicated by the error bars is of a similar level to that of earlier studies obtained by the same method.

For the system developed in this study, the specimen is extremely thin. Small differences in thickness can strongly affect the specimen dry density and i. Therefore, it is necessary to measure the thickness of both the specimen and the test cell before and after the test to confirm the changes in dry density during the test. The variation in dry density due to specimen deformation is in the range of $-0.02 \sim +0.01$ Mg/m^3 when the swelling pressure is measured using a similar device (Wang et al., 2022a). According to Fig. 6, the variation in dry density in the range of $-0.02 \sim +0.01$ Mg/m^3 is small for the k value of a specimen.

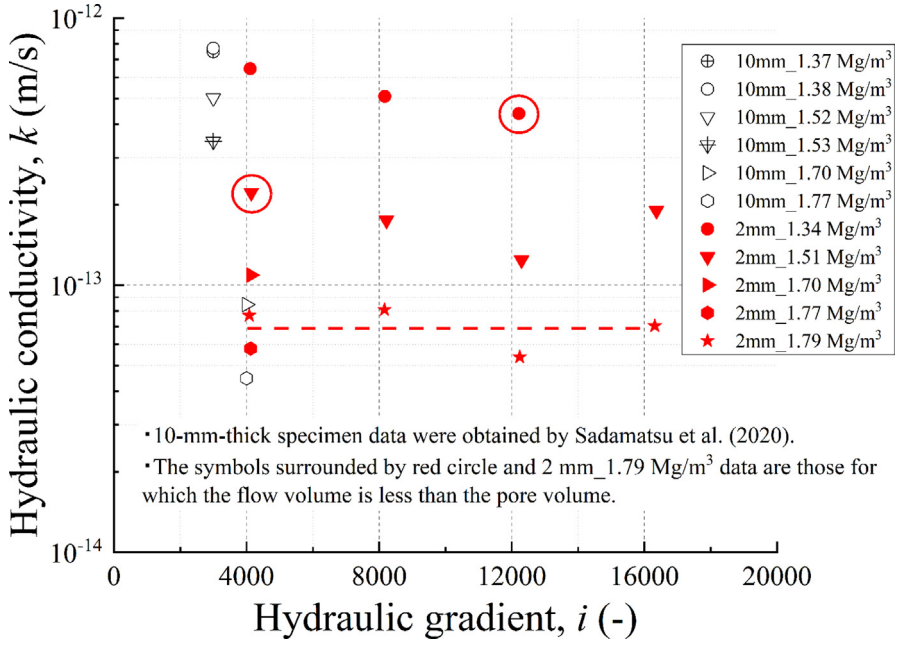

Fig. 5. Relation between hydraulic conductivity and hydraulic gradient in comparison between specimen thicknesses of 2 mm and 10 mm and experimental cases where flow volume is less than pore volume.

Table 3
Comparison of test conditions to previous studies used in Fig. 6.

	Test method	Specimen size (Diameter × Height) (mm)	Approximate hydraulic gradient i (-)	Consolidation pressure (MPa)
This study	Falling head	28 × 2	4,000–16,000	–
Sadamatsu et al., 2020	Falling head	28 × 10	3,000–4,000	–
Komine et al., 2011	High pressure consolidation	60 × 10	–	4.9–9.8
Butsuda et al., 2006	High pressure consolidation	60 × 10	–	5.9–9.8
Hasegawa, 2004	Constant head	60 × 10	1,000–2,000	–

– indicates that there is/are no corresponding data.

4. Conclusion

In this study, a permeability test system was developed with specimens having a thickness of 2 mm and a diameter of 28 mm, and its applicability was evaluated. The hydraulic conductivity was measured using a specimen of bentonite K_V1 compacted to a dry density of 1.34–1.79 Mg/m^3. The effects obtained by varying the hydraulic gradient during the test period on the macroscopic hydraulic behavior of the specimens were investigated. The possibility of shortening the test period using 2-mm-thick specimens was evaluated in terms of the relation between the water flow volume and time. The results showed that, under the same test system and conditions, the time necessary to reach a water flow rate that is equal to the pore volume of the specimen can be reduced considerably, by about one-tenth, compared to the case of 10-mm-thick specimens. Furthermore, the hydraulic gradient set for this study (in the range of 4,000–16,000) did not affect the measured hydraulic conductivity, indicating that the macroscopic hydraulic behavior of the specimens is consistent with Darcy's law. Finally, the relation between the hydraulic conductivity and dry density of the specimens was compared with the results obtained from an earlier study on bentonite K_V1. The results indicated that the hydraulic conductivity obtained in this study is similar to that found in earlier studies, and that the variation in the values was relatively smaller, particularly in terms of the consolidation test results. In conclusion, the results demonstrated that the permeability test system developed in this study can shorten the test period and indicated that it is applicable to permeability measurements of bentonite materials.

Acknowledgments

This study was supported through funding provided by the Research Institute for Environmental Geotechnics. This study was also a part of the outcome of research performed under a Waseda University Grant for Special Research Projects (Project number: 2020C-630). The author thanks Mr. Sadamatsu, West Japan Railway Company, for his cooperation and assistance with the experiments.

References

Achari, G., Joshi, R.C., Bentley, L.R., Chatterji, S., 1999. Prediction of the hydraulic conductivity of clays using the electric double layer theory. Can. Geotech. J. 36, 783–792.

Ahn, H.S., Jo, H.Y., 2009. Influence of exchangeable cations on hydraulic conductivity of compacted bentonite. Appl. Clay Sci. 44, 144–150.

ASTM, 2016. Standards Test Methods for Measurement of Hydraulic Conductivity of Saturated Porous Materials Using a Flexible Wall Permeameter, D5084.

Butsuda, R., Komine, H., Yasuhara, K., Murakami, S., 2006. Advancement of experimentation for measuring hydraulic conductivity of bentonite using high-pressure consolidation test apparatus. J. JSCE 62 (3), 573–578, In Japanese with an English abstract.

Cui, Y.J., Tang, A.M., Loiseau, C., Delage, P., 2008. Determining the unsaturated hydraulic conductivity of a compacted sand-bentonite mixture under constant-volume and free-swell conditions. Phys. Chem. Earth 33, S462–S471.

Dixon, D.A., Graham, J., Gray, M.N., 1999. Hydraulic conductivity of clays in confined tests under low hydraulic gradients. Can. Geotech. J. 36, 815–825.

Gleason, M.H., Daniel, D.E., Eykholt, G.R., 1997. Calcium and sodium bentonite for hydraulic containment application. J. Geotech. Geoenviron. Eng. 123 (5), 438–445.

Hasegawa, T., 2004. Investigation on the effect of seawater to hydraulic property and wetting process of bentonite. CRIEPI research report, N04005, Abiko, Japan: Central Research Institunsute of Electric Power Industry (in Japanese with an English abstract).

ISO, 2004. Soil quality-Determination of hydraulic conductivity if saturated porous materials using a flexible wall permeameter. ISO17313.

Ito, M., Okamoto, M., Suzuki, K., Shibata, M., Sasaki, Y., 1994. Mineral composition analysis of bentonite. ATOMOΣ 36 (11), 1055–1058, In Japanese.

JGS, 2016. Research report by Research Committee on the Utilization and Performance Evaluation Technology of Low-Permeability Soil Materials, pp. 92-97. (In Japanese).

JGS, 2018. Test methods for permeability of low-permeable saturated soils. Japanese Geotechnical Society, JGS0312-2018.

JIS (Japanese Industrial Standards), 2009. Test methods for permeability of saturated soils. JIS A 1218:2009.

JNC (Japan Nuclear Cycle), 1999. Technical reliability of the geological disposal for high-level radioactive waste in Japan – geological disposal research and development. Second compiled – general report. JNC TN 1400 99-020, Tokai, Japan: Japan Nuclear Cycle Development Institute (In Japanese).

Karnland, O., Nilsson, U., Weber, H., Wersin, P., 2008. Sealing ability of Wyoming bentonite pellets foreseen as buffer material – Laboratory results. Phys. Chem. Earth 33, S472–S475.

Kawamura, K., Ichikawa, Y., Nakano, M., Kitayama, K., Kawamura, H., 1999. Swelling properties of smectite up to 90°C in situ X-ray diffraction experiments and molecular dynamic simulations. Eng. Geol. 54, 75–79.

Kobayashi, I., Owada, H., Ishii, T., Iizuka, A., 2017. Evaluation of specific surface area of bentonite-engineered barriers for Kozeny-Carman law. Soils Found. 57, 683–697.

Komine, H., 2008. Theoretical equations on hydraulic conductivities of bentonite-based buffer and backfill for underground disposal of radioactive wastes. J. Geotech. Geoenviron. Eng. 134 (4), 497–508.

Komine, H., 2010. Predicting hydraulic conductivity of sand–bentonite mixture backfill before and after swelling deformation for underground disposal of radioactive wastes. Eng. Geol. 114, 123–134.

Komine, H., 2021. Cation filtration of montmorillonite on hydraulic conductivities of some bentonites in artificial seawater. J. Geotech. Geoenviron. Eng. 147 (5). https://doi.org/10.1061/(ASCE)GT.1943-5606.0002513.

Komine, H., Yasuhara, K., Murakami, S., 2011. Hydraulic conductivity of some bentonites in artificial seawater. J. JSCE 67 (2), 276–287 (In Japanese with an English abstract).

Komine, H., Ogata, N., 1999. Experimental study on swelling characteristics of sand–bentonite mixture for nuclear waste disposal. Soils Found. 39 (2), 83–97.

Komine, H., Watanabe, Y., 2010. The past, present and future of the geo-environment in Japan. Soils Found. 50 (6), 977–982.

Komine, H., Yasuhara, K., Murakami, S., 2009. Swelling characteristics of bentonites in artificial seawater. Can. Geotech. J. 46, 177–189.

Mesri, G., Olson, R.E., 1971. Mechanisms controlling the permeability of clays. Clays Clay Miner. 19, 151–158.

Nishimura, T., Koseki, J., Fredlund, D.G., Rahardjo, H., 2011. Microporous membrane technology for measurement of soil-water characteristic curve. Geotech. Test. J. 35 (1), 1–8.

Pusch, R., 1992. Use of bentonite for isolation of radioactive waste products. Clay Miner. 27, 353–361.

Pusch, R., Yong, R.N., 2006. Microstructure of smectite clays and engineering performance. Taylor & Francis, pp. 107–124.

Sadamatsu, A., Komine, H., Goto, S., Wang, H., Sekiguchi, T., Kitahara, S., Ito, D., Ichikawa, Y., 2020. "Measurements of Hydraulic Conductivity of Compacted Bentonite by the Falling Head Hydraulic Conductivity Test Method and Measuring Method, Proc. (In Japanese), p. 21-1-3-07..

Sellin, P., Leupin, O.X., 2013. The use of clay as an engineered barrier in radioactive-waste management – A review. Clays Clay Miner. 61 (6), 477–498.

Siemens, G., Blatz, J.A., 2006. Development of a hydraulic conductivity apparatus for bentonite soils. Can. Geotech. J. 44, 997–1005.

SKB (Svensk Kärnbränslehantering AB), 2011. Long-term safety for the final repository for spent nuclear fuel at Forsmark, Main report of the SR-Site project. TR-11-01, Stockholm, Sweden: Svensk Kärnbränslehantering AB.

Tanai, K., Kikuchi, H., Nakamura, K., Tanaka, Y., Hironaga, M., 2010. Survey on current status of laboratory test method and experimental consideration for establishing standardized procedure of material containing bentonite. Report of collaboration research between JAEA and CRIEPI, JAEA-Research 2010-025, Tokai, Japan: Japan Atomic Energy Agency. (In Japanese).

Tanaka, Y., Watanabe, Y., 2019. Modelling the effects of test conditions on the measures swelling pressure of compacted bentonite. Soils Found. 59, 136–150.

Wang, H., Shirakawabe, T., Komine, H., Ito, D., Gotoh, T., Ichikawa, Y., Chen, Q., 2019. Movement of water in compacted bentonite and its relation with swelling pressure. Can. Geotech. J. 57, 921–932.

Wang, H., Ito, D., Shirakawabe, T., Ruan, K., Komine, H., 2022a. On swelling behaviours of a bentonite under different water contents. Géotechnique. https://doi.org/10.1680/jgeot.21.00312.

Wang, H., Komine, H., Gotoh, T., 2022b. A swelling pressure cell for X-ray diffraction test. Géotechnique 72 (8), 675–686.

Wang, H., Ruan, K., Harasaki, S., Komine, H., 2022c. Effects of specimen thickness on apparent swelling pressure evolution of compacted bentonite. Soils Found. 62 (1). https://doi.org/10.1016/j.sandf.2021.101099 101099.

Wang, Q., Tang, A.M., Cui, Y.J., Delage, P., Barnichon, J.D., Ye, W.M., 2013. The effects of technological voids on the hydromechanical behavior of compacted bentonite-sand mixture. Soils Found. 53 (2), 232–245.

Watanabe, Y., Tanaka, Y., Nakamura, K., Hironaga, M., 2013. Hydraulic conductivity test for Ca-type bentonite-sand mixture (Part 1) –Test method for reconstituted specimens using rigid-wall permeameter–. CRIEPI research report, N13005, Abiko, Japan: Central Research Institute of Electric Power Industry (In Japanese with an English Abstract).

Yeo, S.S., Shackelford, C.D., Evans, J.C., 2005. Consolidation and hydraulic conductivity of nine model. J. Geotech. Geoenviron. Eng. 131 (10), 1189–1198.